Effect of Thickness of Nanofiber Separator Membrane PAN/PVDF on Supercapacitor's Performance

Silvia Nurlaili Agustina[1], Markus Diantoro[1,2], Hartatiek[1], Nasikhudin[1,2*]

[1]*Department of Physics, State University of Malang, Jalan Semarang No.5, Malang, 65145, East Java, Indonesia*
[2]*Center of Advanced Materials for Renewable Energy, CAMRY, State University of Malang, Jalan Semarang No. 5, Malang 65145, Indonesia*
**Corresponding author:nasikhudin.fmipa@um.ac.id*

Article history:
Received: 17 June 2025 / Received in revised form: 1 July 2025 / Accepted: 4 July 2025
Available online 10 July 2025

ABSTRACT

Separators in supercapacitors have an important role as intermediaries for ions that pass during the charge-discharge process and affect the performance of supercapacitors. Therefore, a comprehensive study is needed related to separator characteristics, including morphology, pore size, diameter, functional group, and electrochemical performance of separator membranes from PAN/PVDF composites. The separator membrane was synthesized using the electrospinning method with thickness variation (2, 4, 6, 8, and 10 layers), followed by supercapacitor fabrication with coin cell device. The resulting membrane was then characterized by Scanning Electron Microscope (SEM) and Fourier Transform Infrared (FTIR). For the result of supercapacitor fabrication with coin cells, Galvanostatic Charge-Discharge (GCD), Cyclic Voltammetry (CV), and Electrochemical Impedance Spectroscopy (EIS) were carried out to determine supercapacitor performance. FTIR results showed that the PAN/PVDF membrane was successfully composites with the addition of new peaks identified as PVDF and PAN at wave numbers 2243.21 and 881 cm^{-1}. The nanofibers formed have diameters ranging from 319.7 to 339.95 nm. The optimum percentage of electrolyte uptake is obtained at membranes that have 6 layers, which is 318.18% and decreases to 173.68% the thickness is 10 layers. In this study, the optimum supercapacitor performance was obtained in the 6 layers variation with a thickness of 75.91 x 10^3 nm with a gravimetric capacitance value is 53.36 F/g, the capacity retention is 88.96% after being tested for 500 cycles, the largest curve area of CV, and an ionic conductivity value is 54 x 10^{-5} S/cm.

Keywords: *Membrane, nanofiber, PAN/PVDF, separator, supercapacitor, thickness.*

I. Introduction

In today's modern life, that increasingly dependent on energy, the amount of electrical energy demand also increasing. Researchers predict that there will be an energy crisis caused by an imbalance between demand and existing energy supply [1]. Energy storage devices have an important effect on the process of reducing dependence on fossil fuels, that are less environmentally friendly [2]. Lithium-ion batteries are one of the most popular energy storage devices, but lithium is a toxic material that can damage the environment [3]. To overcome this and see the many pollution issues due to greenhouse gases, it is necessary to develop alternative energy sources that are efficient and environmentally friendly for the future [4]. Supercapacitors can be one of the efficient energy storage alternatives for now because they are able to store energy through electrical double layers and faradic reactions,

DOI: 10.17977/um016v9i12025p228

have high density when compared to batteries, have good stability, fast charge cycles, great capacitance, and longer cycle life [5], [6].

The components of supercapacitors consist of electrodes, electrolytes, and separators [7]. Each component in supercapacitors has an important role in improving supercapacitor performance, including separators [8]. A good separator is a separator that has chemical stability, temperature, shape, ability to absorb ions, good ionic conductivity, and a stable cycle [9]. For now, there are still many commercial separators that experience high thermal shrinkage, limited ionic conductivity, low porosity, and poor durability [10]. Therefore, it is necessary to develop a membrane separator that has high porosity, low resistance, good ion-absorbing ability, safer, and stable [11]. The thickness of the separator also affects the performance of the supercapacitor, where the thickness will affect the length of ions that pass during the charge-discharge process [12]. Separators with a thickness that is too thin will make the supercapacitor's performance decrease, and will experience a short circuit [13]. While the separator with a thickness that is too thick inhibits the ion transfer process, so that the electrochemical intensity and capacity of the supercapacitor will decrease. Therefore, the separator must have an ideal thickness to achieve optimum supercapacitor performance [14].

Electrospinning is one method to produce nano-sized membranes for a separator application [15]. Nanofibers produced from the electrospinning method have a large surface area and high porosity [16]. Several studies have shown that polyacrylonitrile (PAN) and polyvinylidene fluoride (PVDF) polymers were successfully synthesized using the electrospinning method [17], [18]. PAN has good thermal resistance, high chemical stability, and good mechanical properties. While PVDF has high electrochemical stability properties. Therefore, PAN/PVDF membrane can be a good separator when applied to supercapacitors. Some studies also show that separators with variations in thickness show an influence on the performance of the membrane when applied to supercapacitors [19], [20].

Zheng *et al*. tested the PAN/PVDF/PAN separator membrane and obtained a porosity percentage of 63.44% at a thickness of 23 x 10^3 nm [21]. Wen *et al*. also reported that the ionic conductivity value increased by 100% as the thickness of the separator decreased by 2 x 10^{-5} nm [20]. Gilshteyn *et al*. reported that PVA synthesized by the electrospinning method obtained the smallest thickness of 1.5 x 10^{-5} nm and caused a higher resistance value [22]. Several previous studies have shown that separator thickness plays an important role in determining the electrochemical performance of supercapacitors. However, no studies have focused on the thickness of PAN/PVDF separators in supercapacitors. Given that PAN/PVDF offers a promising combination of mechanical robustness and electrochemical compatibility. Therefore, this study aims to evaluate the electrochemical behavior of PAN/PVDF membranes with various thicknesses in supercapacitor applications.

II. Material and Methods

1. Materials

The materials needed in this research are polyacrylonitrile (PAN with Mw 150,000 g/mol), polyvinylidene fluoride (PVDF with Mw 180,000 g/mol), N,N-dimethylformamide (DMF) as solvent were purchased from Sigma Aldrich, activated carbon (AC, Thailand), carbon black (CB, Belgium), LA 133 binder (Belgium), Et_4NBF_4 electrolyte, DI water, ethanol, and set coin cell type LIR2032 (China).

2. Preparation of PAN/PVDF Nanofiber Membrane

The composite manufacturing stage begins with dissolved 0.32 g of PAN in 4.6 ml of DMF with magnetic stirrer at 800 rpm and 80°C for 1 hour. Then, 0.08 g of PVDF was added and stirred again at 1000 rpm and 80°C for 2 hours. After that, the solution was sonicated for 1 hour. Next, it was stirred again at 1000 rpm at room temperature for 20 hours. After 20 hours, the solution was reheated at 50°C for 20 minutes. Before electrospinning, stirred again the composite at 1000 rpm at room temperature for 30 minutes. The homogeneous PAN/PVDF composite solution was put into a 10 ml syringe with a 24½ syringe needle cut off at the end. The electrospinning device was set to a voltage of 9 kV and flow rate of 20. The nanofibers were then oven at 75°C for 5 h. The membrane will be varied by layer to obtain different thicknesses. To make it easier, the samples were named by PP2, PP4, PP6, PP8, and PP10 for 2, 4, 6, 8, and 10 membrane layers, respectively.

3. Preparation for AC-CB electrode

The AC-CB electrode paste was prepared by dissolved 1 g of LA 133 binder with 2 mL DI water and stirred using magnetic stirrer at 200 rpm for 30 minutes. Then, add 0.1 g of CB and stirred at 200 rpm for 30 minutes. Then, add 0.9 g of AC and stirred at 200 rpm for 30 minutes. Then, the sample was stirred again using a magnetic stirrer at 300 rpm for 24 hours. The obtained paste was then deposited on aluminum foil using a doctor blade with a thickness of 20 μm. Then, it was annealed for 2 hours at 80°C.

4. Fabrication of Supercapacitor

After synthesizing each component of the supercapacitor, the next step is fabrication. In this study, supercapacitor fabrication used coin cell device. The supercapacitor arrangement with coin cells is shown in Figure 1.

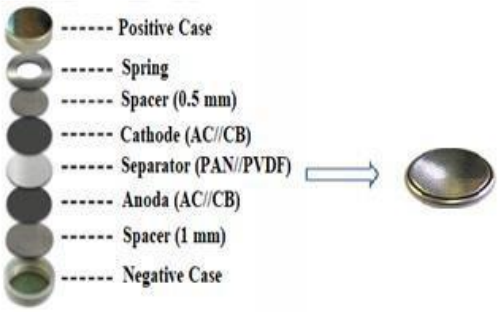

Fig 1. Supercapacitor assembled in this study

5. Characterization and Calculation

The morphology of the membrane was characterized using Scanning Electron Microscopy-cross section (SEM, FEI Inspect-S50). Fourier Transform Infra-Red (FTIR, Shimadzu IR Prestige 21) was performed to determine the functional group in the wavenumber range of 4000 – 500 cm^{-1}. To determine the electrolyte uptake ability (%), the membranes were immersed in Et_4NBF_4 electrolyte for 2 hours. The mass before and after immersion was recorded to calculate the electrolyte uptake ability (%), as shown in Eq. (1).

$$Electrolyte\ Uptake\ (\%) = \frac{W-Wo}{Wo} \times 100 \quad (1)$$

The electrochemical performance of supercapacitor was characterized using Galvanostatic Charge-Discharge (GCD, Solarton 1286). The data obtained from GCD are

the values of gravimetric capacitance (Cg), energy density (E), power density (P), and capacity retention. The gravimetric capacitance, energy density, power density, and capacity retention were calculated using Eq. (2), (3), (4), and (5), respectively.

$$Cg = \frac{4I\Delta t}{m\Delta V} \quad (2)$$

$$E = \frac{1}{8}\frac{C\Delta V^2}{3.6} \quad (3)$$

$$P = \frac{3600E}{\Delta t} \quad (4)$$

$$Capacity\ Retention\ (\%) = \frac{Cn}{Co} \times 100 \quad (5)$$

Where Cg is gravimetric capacitance, V is the voltage, t is the time, m is the mass of electrode, Cn is the capacitance after n cycles, and Co is the initial capacitance.

Furthermore, electrochemical performance of supercapacitor was characterized by cyclic voltammetry (CV) and electrochemical impedance spectroscopy (EIS) using Gamry. From EIS, the ionic conductivity value was determined using Eq. (6).

$$\sigma = \frac{d}{Rct \times A} \quad (6)$$

Where d is the thickness of the membrane, Rct is the charge transfer resistance, and A is the membrane area.

III. Results and Discussions

1. Functional Groups of PAN/PVDF Separator Membranes

Figure 2 shows that the IR spectra of PAN and PAN/PVDF are almost similar, especially at wavenumber 2243.21 (C≡N bond stretching vibration), 2939.51 (C-H stretching vibration), and 1073.35 cm^{-1}, which are typical of PAN spectra.

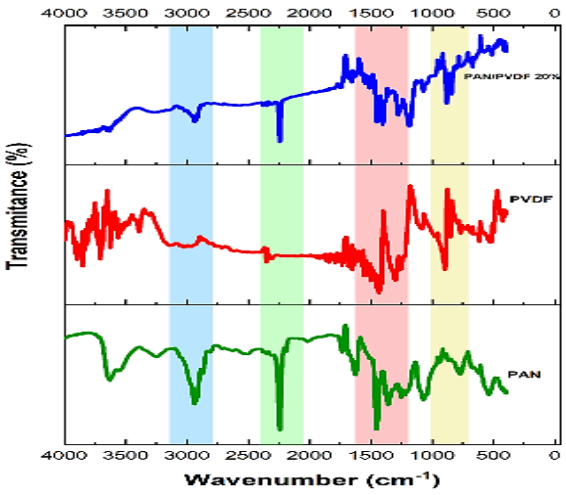

Fig 2. IR spectra of PAN, PVDF, and PAN/PVDF

The IR spectrum graph of PAN is almost similar to PAN/PVDF because the composition is dominated by PAN [23]. The IR spectrum of PAN/PVDF also found a peak that is characteristic of PVDF at wave number of 881.11 cm^{-1}, which is a C-F stretching vibration bond. Furthermore, the PAN/PVDF composite absorption peaks experience a slight shift to smaller wave numbers, indicating the presence of intermolecular interactions. The

interaction is dipole-dipole attraction, which causes a slight weakening of bonds [24]. These results confirm that the PAN and PVDF composite results still obtained both polymers with more PAN concentration than PVDF. Table 1 shows the characteristics of IR absorption of PAN, PVDF, and PAN/PVDF.

Table 1. Comparison of IR spectra of PAN/PVDF membrane

Wavenumber (cm^{-1})				Characteristics
PAN	PVDF	PAN/PVDF	Reference	
-	881.11	881.46	~880	C-F stretching vibration [17]
1074.35	1078.2	1074.35	~1190 – 1390	C-H group [25]
-	1404.17	1406.75	~1401	C-H bond bending vibration [26]
2243.21	-	2241.28	~2238 – 2243	C≡N nitrile group stretching vibration [27]
2939.51	-	2938.15	~2943	C-H stretching vibration [26]

Figure 3 shows that at wave numbers 2243.21 cm^{-1} and 881 cm^{-1}, no shift is observed, indicating that each variation still contains PAN and PVDF polymers in the composite. In Figure 3, it can also be observed that there are differences in absorbance at wave numbers 2243.21 cm^{-1} and 881 cm^{-1} in each variation. The thicker the separator membrane, the greater the absorbance value obtained. This shows that the thicker the separator membrane, the more PAN and PVDF polymers contained in it [28].

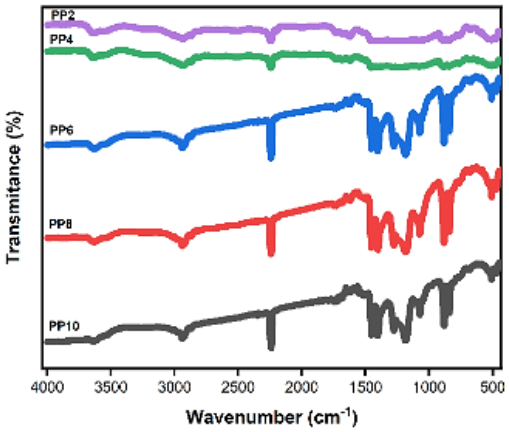

Fig 3. IR spectra of PAN/PVDF membranes with various thicknesses

2. *Morphology and Thickness of PAN/PVDF Separator Membrane*

Figure 4a-e shows the morphology of PAN/PVDF membrane with varying thickness. The SEM images show that the morphology of fiber is formed without beads. Table 2 shows the diameter of fibers in the range of 319.7 nm to 339.95 nm. The fiber diameter range is not far adrift because the same polymer concentration is used in all variations. This is in accordance with the theory that the diameter of the fiber depends on the polymer concentration used, flow rate, voltage, collector shape, and the distance between the collector and the needle tip during electrospinning [29]. The results of the measurement of the diameter of the fiber produced are in accordance with the theory of nanofiber diameter size, ranging from 100 nm to 500 nm [30].

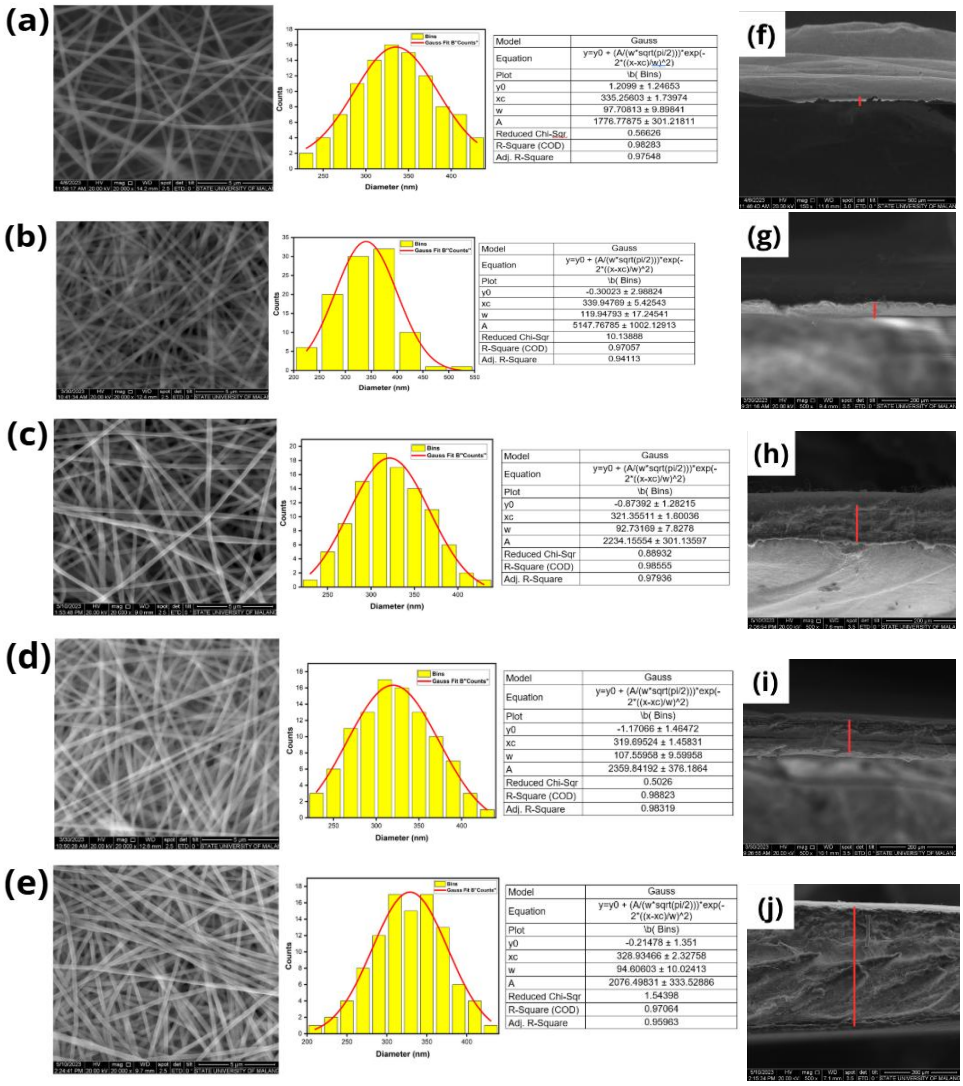

Fig 4. Morphology from SEM and normal distribution of (a) PP2; (b) PP4; (c) PP6; (d) PP8; (e) PP10 and cross-section of (f) PP2; (g) PP4; (h) PP6; (i) PP8; (j) PP10.

Table 2. Result from SEM and electrolyte uptake ability of PAN/PVDF membranes

Sample	Average thickness (nm)	Average fiber diameter (nm)	Average pore size (nm)	Electrolyte uptake (%)
PP2	13.97×10^3	335.26 ± 1.74	537.96	262.5
PP4	32.67×10^3	339.95 ± 5.45	165.81	280.0
PP6	75.91×10^3	321.36 ± 1.60	142.28	318.2
PP8	86.31×10^3	319.70 ± 1.46	129.77	240.0
PP10	151.56×10^3	328.93 ± 2.33	94.49	173.7
Whatman	-	-	-	128.6

Figure 4f-j shows the cross-section of the nanofiber membranes. The results of analysis using ImageJ software obtained thicknesses ranging from 13.97 to 151.46 x 10^3 nm, as presented in Table 2. This shows the success of varying thickness variations with the addition of layers. Pore size measurement results are in the range of 94.49 - 537.96 nm. The thicker

of PAN/PVDF separator membrane, the smaller pore size due to the overlap in each layer between fibers and pores. The ideal pore size for a separator is <1000 nm [31]. The results obtained in this study support that the separator produced is ideal according to its pore size. Separator serves as a medium for ion transfer in supercapacitors; therefore, the pore size must be uniform and can transverse the electrolyte ions [32]. In this study, using Et_4NBF_4 electrolyte, which has Et_4N^+ and BF_4^- with diameters of 0.343 and 0.229 nm, respectively [3]. It shows that the pore size produced in this study is larger than the diameter of ions in the electrolyte, which means that ion mobility can move smoothly [33].

Besides pore size, separator must also have good electrolyte uptake ability. High electrolyte uptake ability can increase the ionic conductivity, thereby facilitating the rapid transport of ions in supercapacitor [34]. The percentage of electrolyte uptake ability is shown in Table 2. Thinner separators (PP2, PP4, and PP6) have a higher electrolyte uptake ability than thicker separators (PP8 and PP10). The optimum electrolyte uptake ability was obtained in PP6, reaching 318.18%. The decrease in electrolyte uptake ability observed in PP8 and PP10 was 240% and 173.68%, respectively. Membrane separators that have many pores but are too thin will have a tendency to absorb less of electrolyte. Similarly, the membrane is too thick, resulting in limited access to electrolyte ions to be absorbed [35]. PP6 shows a higher electrolyte uptake ability than the Whatman as a commercial separator. PAN/PVDF membrane has a stronger interaction with electrolyte molecules, thus accelerating the infiltration and retention of electrolytes in the membrane pores.

3. Electrochemical Performance of Supercapacitor

Supercapacitor performance was characterized by Cyclic Voltammetry (CV), Electrochemical Impedance Spectroscopy (EIS), and Galvanostatic Charge Discharge (GCD) using two-electrode system. Good supercapacitor performance is evaluated based on several electrochemical parameters, including high specific capacitance values, energy density, power density, high capacity retention, and high ionic conductivity value.

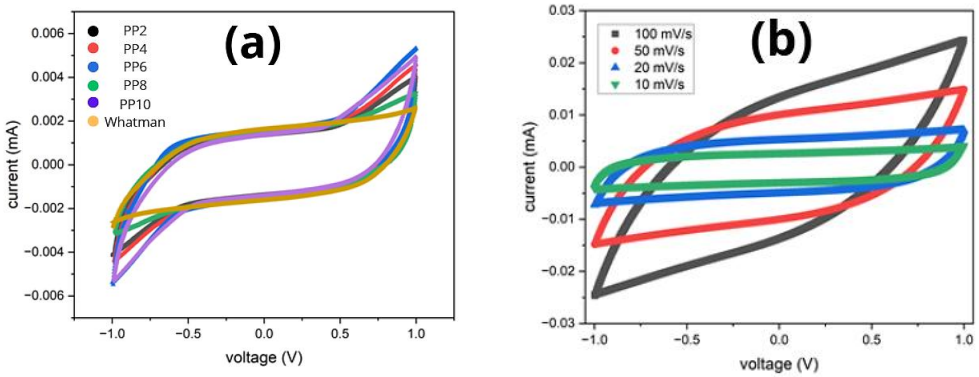

Fig 5. Cyclic voltammograms of (a) PAN/PVDF membranes at scan rate of 5 mV/s, (b) PP6 sample at scan rates of 10, 20, 50, and 100 mV/s

Figure 5a shows the voltammetry graph for all samples with scan rate of 5 mV/s. All curves are all the same shape, which is semi-rectangular, indicating that the electrode is electric double layer capacitor (EDLC) type due to the use of carbon-based material for electrode [36]. PP6 has the largest curve area, indicating that the separator PP6 provides optimum charge-discharge cycles with minimum degradation. The largest curve area also indicates a high charge storage capacity, which means a larger specific capacitance [37]. Figure 5b shows the CV curve of PP6 at various scan rates (10, 20, 50, and 100 mV/s). All

curves were formed without any discontinuity, indicating that charge diffusion is excellent with stable electrochemical performance [38]. When the scan rate is 50 – 100 mV/s, the curve becomes more pointed at the end due to insufficient diffusion of electrolyte ions [39].

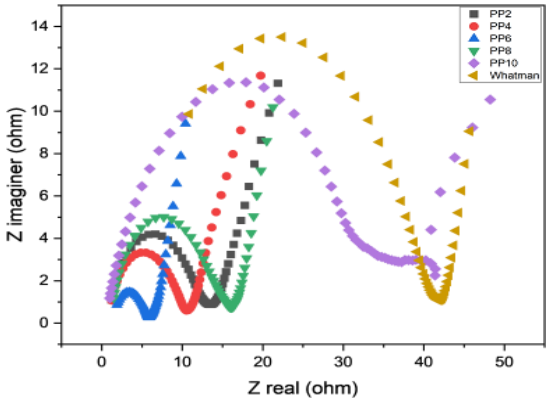

Fig 6. Nyquist plot of PAN/PVDF membranes

Figure 6 shows the Nyquist plot for all samples, which consists of a semicircle followed by a linear tail. The diameter of semicircle represents the charge transfer resistance (Rct), which indicates the resistance to electron transfer at the interface of the electrode and electrolyte [40]. The smallest diameter is observed in PP6, with an Rct value of 4.41 ohm, and increased when the separator gets thicker and thinner. Membranes with nanoscale diameters and optimum pore sizes have a high specific surface area. The high specific surface area provides a greater number of electrochemically active sites, thereby facilitating more efficient charge storage through electric double layer formation at the electrode–electrolyte interface. It can reduce the Rct value due to its ability to create more efficient ion and electron transport pathways [41]. Lower Rct values indicate more efficient electron transfer, thus improving the supercapacitor performance [42]. The thicker of separator, the longer ion diffusion distance. This makes ion transport slower, making it more difficult for ions to reach the electrode interface where the chemical reaction takes place. This is in accordance with Fick's law, which states that ion diffusion time is directly proportional to the square of the distance [43]. A separator that's too thick requires a longer ion transport and capacitive response time, thus increasing the Rct value. The thinner of separator, the amounts of electrolyte that can be absorbed is also less. This reduces the number of ions available to move during the charge and discharge process. The electrode interface will lack electrolyte, causing an increase in Rct value. It can be related to the highest electrolyte uptake ability also obtained by PP6. The average pore size of PP6 is 142.28 nm, which means the pore size is ideal for PAN/PVDF separator. The Rct value obtained by PP6 is also smaller when compared with Whatman as commercial separator.

Based on calculations using Eq. (6), the ionic conductivity values of the PAN/PVDF separator with varying thickness are presented in Table 3. PP6 has the highest ionic conductivity when compared to other samples and commercial separator (Whatman). Ionic conductivity value of PP6 is equal to 54×10^{-5} S/cm and increases when the separator gets thicker. The smaller Rct value means a greater ionic conductivity value because it reflects a more efficient charge transfer process, allowing ions to move freely through when crossing the electrode-electrolyte interface [44]. Comparison of the results in this study with previous study is summarized in Table 4. Among all the studies presented in Table 4, the ionic conductivity value in this study remains higher, which indicates that the PAN/PVDF membrane was successfully applied in supercapacitor.

Table 3. Rct and ionic conductivity values of PAN/PVDF membranes

Sample	Rct (Ω)	σ (S/cm)
PP2	12.12	3.7×10^{-5}
PP4	9.53	10.9×10^{-5}
PP6	4.41	54.0×10^{-5}
PP8	15.01	18.3×10^{-5}
PP10	40.16	12.0×10^{-5}
Whatman	31.66	7.1×10^{-5}

Table 4. Comparison of ionic conductivity values with previous studies

Separator	Electrode	Electrolyte	Thickness (nm)	σ (S/cm)	Reference
PAN	$LiFePO_4$	-	22.0×10^3	0.25×10^{-5}	[21]
PVDF	Stainless steel	$EMIMBF_4$	150.0×10^3	2.02×10^{-5}	[45]
PVA/SiO_2	-	-	20.7×10^3	0.01×10^{-5}	[46]
PVA/TEOS	-	-	54.6×10^3	0.01×10^{-5}	[46]
PAN/PVDF 20%	AC-CB	Et_4NBF_4	75.9×10^3	54.0×10^{-5}	This work

Figure 7 shows that the PP6 sample with a thickness of 75.91 x 10^3 nm has the longest discharge time, reaching 230 seconds. The discharge time obtained on the PP6 sample is longer than the Whatman commercial separator. This is attributed to the lower electrolyte ion transfer resistance, as confirmed by results of EIS.

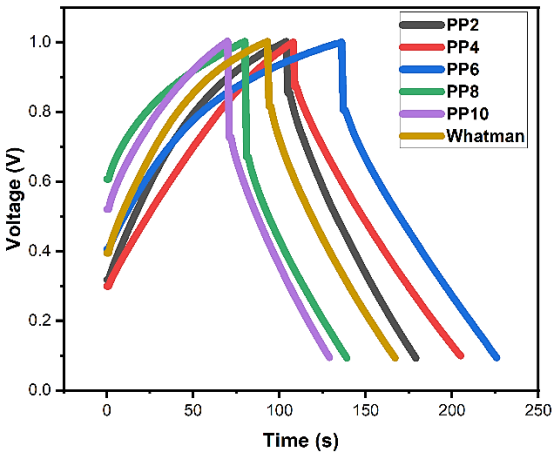

Fig 7. Electrochemical performance based on GCD test of PAN/PVDF membranes

Table 5 shows the gravimetric capacitance, energy density, and power density of supercapacitor with PAN/PVDF membranes. The optimum gravimetric capacity value is observed in PP6, reaching 53.36 F/g. Thinner membranes (PP2 and PP6) obtained gravimetric capacitance values of 45.79 F/g and 45.85 F/g, while thicker membranes (PP8 and PP10) obtained gravimetric capacitance values of 43.05 F/g and 41.27 F/g. The thicker PAN/PVDF separator membrane gets a lower gravimetric capacitance value when compared

to the membrane with a thinner thickness. This is in accordance with the theory that the size of the separator thickness should be ideal so as to get the maximum gravimetric capacity value [47]. A thicker separator makes too much active material not directly adjacent to the electrolyte, so that the electrochemical intensity and capacity of the supercapacitor will decrease. Conversely, if the separation membrane is too thin, the performance of the supercapacitor will decrease and cause a short circuit [48].

Table 5. Energy discharge of PAN/PVDF membranes

Sample	Cg ($F.g^{-1}$)	E ($Wh.kg^{-1}$)	P ($W.kg^{-1}$)
PP2	45.79	0.53	32.96
PP4	45.85	0.95	35.57
PP6	53.36	0.94	37.97
PP8	43.05	0.75	36.84
PP10	41.27	0.60	37.05
Whatman	45.24	0.91	44.34

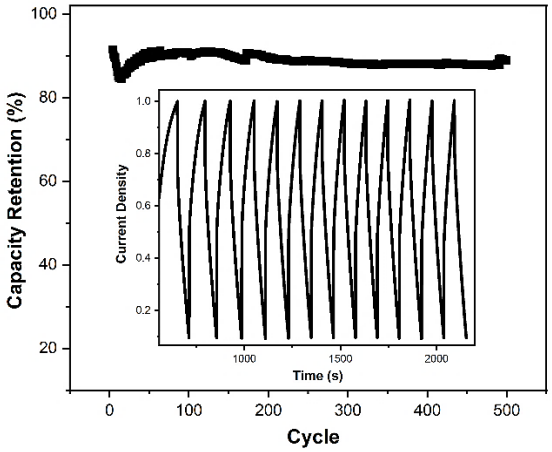

Fig 8. Capacity retention of PP6

Table 6. Comparison of capacitance values with previous studies

Separator	Electrode	Electrolyte	Thickness (nm)	Cg (F/g)	Reference
PE	MnO_2	K_2SO_4	2×10^6	4.32	[19]
PE	MnO_2	K_2SO_4	35×10^6	3.68	[19]
PVDF	AC-PTFE-CB	Et_4NBF_4	-	39.50	[49]
PAN/PVDF 20%	AC-CB	Et_4NBF_4	0.0759×10^6	53.36	This work

The capacity retention of the PP6 sample is shown in Figure 8. The capacity retention obtained is 88.96% after being tested for 500 cycles. It shows that the PP6 sample with a thickness of 75.91 x 10^3 nm has good resistance and shows that the membrane works efficiently as a separator in supercapacitors. Table 6 shows the comparison of gravimetric capacitance values in this study with previous studies using polymers. Among all the studies

in Table 6, the gravimetric capacitance in this study remains higher. That indicates that the PAN/PVDF separator was successfully applied in supercapacitor.

IV. Conclusions

This study concluded that the PAN/PVDF composite was successfully carried out, indicated by the presence of typical peaks of PAN and PVDF in the results of the composite IR spectrum at wave numbers 2243.21 cm^{-1} and 881 cm^{-1} as C≡N nitrile group stretching vibration and C-F stretching vibration. The absorbance seen in the graph shows a higher value when the thickness increases. The morphology of the nanofibers obtained did not show any beads in all variations, with fiber diameter in the range of 319.7 – 339.95 nm, and pore size obtained ranged from 94.496 to 537.96 nm, where the thicker the membrane, the smaller the pore size produced. The measurement of optimum electrolyte uptake ability in the PP6 sample is 318.18%. Electrochemical performance shows the results of GCD characterization on PP6 samples produce optimum results of 53.36 F/g with a capacity retention of 88.96% after 500 cycles. The CV test results show that the largest curve area is shown in sample PP6, and from the EIS test, the optimum ion conductivity value was obtained in the PP6 sample of 54 x 10^{-5} S/cm. The electrochemical performance results showed that the PP6 sample with a thickness of 75.91 x 10^3 nm had the most optimum value when compared to other samples and the Whatman commercial separator. Separator must also have good electrolyte uptake ability. Membranes with the highest electrolyte uptake ability can increase the ionic conductivity, thereby facilitating the rapid transport of ions in supercapacitors, and can increase the specific capacitance value. This research implies that PAN/PVDF membrane with a thickness of 75.91 × 10^3 nm is potential for use in supercapacitor applications. The optimized thickness separator membrane has the potential to be applied in supercapacitors that require high stability, such as energy storage devices for electric vehicles, large-scale energy storage systems, or flexible electronic devices. However, the thickness variation in this study was achieved by layering the membrane rather than by adjusting electrospinning parameters. Therefore, further research needs to systematically control the membrane thickness through electrospinning process parameters for improved consistency and scalability.

Acknowledgment

We would like to thank the State University of Malang, and all colleagues who have assisted in carrying out this research activity through PNBP funding.

References

[1] M. Mirzaeian, Q. Abbas, A. Ogwu, P. Hall, M. Goldin, and M. Mirzaeian *et al*., "Electrode and electrolyte materials for electrochemical capacitors," *Int. J. Hydrogen Energy*, vol. 42, no. 40, pp. 25565–25587, 2017, doi: 10.1016/j.ijhydene.2017.04.241.

[2] M. Y. Bhat, S.A. Hashmi, M. Khan, D. Choi, and A. Qurashi, "Frontiers and recent developments on supercapacitor's materials, design, and applications: Transport and power system applications," *J. Energy Storage*, vol. 58, p. 106104, Feb. 2023, doi: 10.1016/J.EST.2022.106104.

[3] M. Diantoro, I. Istiqomah, Y. Al Fath, N. Mufti, N. Nasikhudin, and W. Meevasana *et al*., "Hierarchical activated carbon–MnO_2 composite for wide potential window asymmetric supercapacitor devices in organic electrolyte," *Micromachines*, vol. 13, no. 11, 2022, doi: 10.3390/mi13111989.

[4] E.K. Addo, A.T. Kabo-Bah, F.A. Diawuo, and S.K. Debrah, "The role of nuclear energy in reducing greenhouse gas (GHG) emissions and energy security: A systematic review," *Int. J. Energy Res.*, 2023, doi: 10.1155/2023/8823507.

[5] R. Arthi, V. Jaikumar, and P. Muralidharan, "Development of electrospun PVdF polymer membrane as separator for supercapacitor applications," *Energy Sources, Part A Recover. Util. Environ. Eff.*, vol. 44, no. 1, pp. 2294–2308, 2022, doi: 10.1080/15567036.2019.1649746.

[6] O. Hubert, N. Todorovic, and A. Bismarck, "Towards separator-free structural composite supercapacitors," *Compos. Sci. Technol.*, vol. 217, p. 109126, Jan. 2022, doi: 10.1016/J.COMPSCITECH.2021.109126.

[7] D. Xu, G. Teng, Y. Heng, Z. Chen, and D. Hu, "Eco-friendly and thermally stable cellulose film prepared by phase inversion as supercapacitor separator," *Mater. Chem. Phys.*, vol. 249, no. December 2019, p. 122979, 2020, doi: 10.1016/j.matchemphys.2020.122979.

[8] C. Zhao, J. Niu, C. Xiao, Z. Qin, X. Jin, and W. Wang *et al*., "Separator with high ionic conductivity and good stability prepared from keratin fibers for supercapacitor applications," *Chem. Eng. J.*, vol. 444, p. 136537, Sep. 2022, doi: 10.1016/J.CEJ.2022.136537.

[9] J. Xing, S. Bliznakov, L. Bonville, M. Oljaca, and R. Maric, "A review of nonaqueous electrolytes, binders, and separators for Lithium-ion batteries," *Electrochemical Energy Reviews*., vol. 5, no. 4, 2022, doi: 10.1007/s41918-022-00131-z.

[10] S. Wu, J. Ning, F. Jiang, J. Shi, and F. Huang, "Ceramic nanoparticle-decorated melt-electrospun PVDF nanofiber membrane with enhanced performance as a Lithium-ion battery separator," *ACS Omega*, vol. 4, no. 15, pp. 16309–16317, 2019, doi: 10.1021/acsomega.9b01541.

[11] L. Li and Y. Duan, "Engineering Polymer-Based Porous Membrane for Sustainable Lithium-Ion Battery Separators," *Polymers (Basel).*, vol. 15, no. 18, 2023, doi: 10.3390/polym15183690.

[12] M. Beg, K.M. Alcock, A. Titus Mavelil, D. O'Rourke, D. Sun, and K. Goh *et al*., "Paper supercapacitor developed using a manganese dioxide/carbon black composite and a water hyacinth cellulose nanofiber-based bilayer separator," *ACS Appl. Mater. Interfaces*, vol. 15, no. 44, pp. 51100–51109, 2023, doi: 10.1021/acsami.3c11005.

[13] M. Yaseen, M.A.K. Khattak, M. Humayun, M. Usman, S.S. Shah, and S. Bibi *et al*., "A review of supercapacitors: Materials design, modification, and applications," *Energies*, vol. 14, no. 22, pp. 1–40, 2021, doi: 10.3390/en14227779.

[14] G. Qi, S. Nguyen, D.B. Anthony, A.R.J. Kucernak, M.S.P. Shaffer, and E.S. Greenhalgh, "The influence of fabrication parameters on the electrochemical performance of multifunctional structural supercapacitors," *Multifunct. Mater.*, vol. 4, no. 3, 2021, doi: 10.1088/2399-7532/ac1ea6.

[15] M. Ma, H. Zhou, S. Gao, N. Li, W. Guo, and Z. Dai, "Analysis and prediction of electrospun nanofiber diameter based on artificial neural network," *Polymers (Basel).*, vol. 15, no. 13, 2023, doi: 10.3390/polym15132813.

[16] X. Cao, W. Chen, P. Zhao, Y. Yang, and D.G. Yu, "Electrospun porous nanofibers: pore−forming mechanisms and applications for photocatalytic degradation of organic pollutants in wastewater," *Polymers (Basel)*, vol. 14, no. 19, 2022, doi: 10.3390/polym14193990.

[17] A.I. Yardimci, M. Kayhan, A. Durmus, M. Aksoy, and O. Tarhan, "Synthesis and air permeability of electrospun PAN/PVDF nanofibrous membranes," *Res. Eng. Struct. Mater.*, vol. 8, no. 2, pp. 223–231, 2022, doi: 10.17515/resm2022.357na1027.

[18] A.W. Jatoi, P.K. Gianchandani, I.S. Kim, and Q.Q. Ni, "Sonication induced effective approach for coloration of compact polyacrylonitrile (PAN) nanofibers," *Ultrason. Sonochem.*, vol. 51, pp. 399–405, 2019, doi: 10.1016/j.ultsonch.2018.07.035.

[19] P. Mandake and P.B. Karandikar, "Effect of separator thickness variation for supercapacitor with polyethylene separator material," *J. Sci. Res. Sci. Eng. Technol.*, vol. 2, no. 2, pp. 967–971, 2016.

[20] J. Wen, K. Xu, R. Li, D. Lv, Y. Cui, and Y. Chen *et al*., "Electrospun flexible aluminum silicate nanofibers as a flame-resistant separator for the high performance supercapacitor," *Ionics (Kiel).*, vol. 28, no. 1, pp. 433–442, 2022, doi: 10.1007/s11581-021-04329-x.

[21] Y. Zheng, R. Zhou, H. Zhao, and F. Ye, "Oriented PAN/PVDF/PAN laminated nanofiber separator for lithium-ion batteries," *Text. Res. J.*, vol. 92, 2022, doi: 10.1177/00405175211005027.

[22] E.P. Gilshteyn, D. Amanbayev, A.S. Anisimov, T. Kallio, and A.G. Nasibulin, "All-nanotube stretchable supercapacitor with low equivalent series resistance," *Sci. Rep.*, vol. 7, no. 1, pp. 1–9, 2017, doi: 10.1038/s41598-017-17801-4.

[23] R.M. Ahmed, "Surface characterization and optical study on electrospun nanofibers of PVDF/PAN blends," *Fiber Integr. Opt.*, vol. 36, no. 1–2, pp. 78–90, 2017, doi: 10.1080/01468030.2017.1280098.

[24] P. Deb, T. Haldar, S.M. Kashid, S. Banerjee, S. Chakrabarty, and S. Bagchi, "Correlating nitrile IR frequencies to local electrostatics quantifies noncovalent interactions of peptides and proteins," *J. Phys. Chem. B*, vol. 120, no. 17, pp. 4034–4046, 2016, doi: 10.1021/acs.jpcb.6b02732.

[25] A. Anvari, A.A. Yancheshme, F. Rekaabdar, M. Hemmati, M. Tavakolmoghadam, and A. Safekordi, "PVDF/PAN blend membrane: Preparation, characterization and fouling analysis," *J. Polym. Environ.*, vol. 25, no. 4, pp. 1348–1358, 2017, doi: 10.1007/s10924-016-0889-x.

[26] H. Zhu, X. Deng, V.V. Yakovlev, and D. Zhang, "Dynamics of CH/n hydrogen bond networks probed by time-resolved CARS spectroscopy," *Chem. Sci.*, pp. 14344–14351, 2024, doi: 10.1039/d4sc03985h.

[27] Y.A.Y.A. Mohammed, F. Ma, L. Liu, C. Zhang, H. Dong, and Q. Wang *et al*., "Preparation of electrospun polyvinylidene fluoride/amidoximized polyacrylonitrile nanofibers for trace metal ions removal from contaminated water," *J. Porous Mater.*, vol. 28, no. 2, pp. 383–392, 2021, doi: 10.1007/s10934-020-00995-w.

[28] B.E.K. Dewi, Pranoto, O.A. Saputra, and E. Pramono, "Performance improvement polyvinylidene fluoride (PVDF) mordenite membranes for oil-in-water emulsion separation," *ALCHEMY*, vol. 20, no. 2, pp. 226–237, 2024, doi: 10.20961/alchemy.20.2.82146.226-237.

[29] H. Gade, S. Nikam, G.G. Chase, and D.H. Reneker, "Effect of electrospinning conditions on β-phase and surface charge potential of PVDF fibers," *Polymer (Guildf).*, vol. 228, no. February, p. 123902, 2021, doi: 10.1016/j.polymer.2021.123902.

[30] J. Liu, J. Wang, L. Zhu, X. Chen, Q. Ma, and L. Wang *et al*., "A high-safety and multifunctional MOFs modified aramid nanofiber separator for lithium-sulfur batteries," *Chem. Eng. J.*, vol. 411, no. December 2020, p. 128540, 2021, doi: 10.1016/j.cej.2021.128540.

[31] Z. Wang, H. Ren, B. Wang, S. Yang, B. Wu, and Y. Zhou *et al*., "Microfiber/nanofiber/attapulgite multilayer separator with a pore-size gradient for high-performance and safe lithium-ion batteries," *Molecules*, vol. 29, no. 14, 2024,

doi: 10.3390/molecules29143277.

[32] J. Bates, F. Markoulidis, C. Lekakou, and G.M. Laudone, "Design of porous carbons for supercapacitor applications for different organic solvent-electrolytes," *J. Carbon Res.*, vol. 7, no. 1, p. 15, 2021, doi: 10.3390/c7010015.

[33] J. Lee, J. Yoon, J. Jeon, Y. Hong, S.G. Oh, and H. Huh, "Electrospun PVDF-HFP/PAN bicomponent nanofibers as separators in lithium-ion batteries with high thermal stability and electrolyte wettability," *Korean J. Chem. Eng.*, vol. 40, no. 8, pp. 1901–1911, 2023, doi: 10.1007/s11814-023-1486-z.

[34] H. Wu, H. Huang, Y. Xu, F. Xu, and X. Zhang, "Ultrathin separator with efficient ion transport and superior stability prepared from cotton cellulose for advanced supercapacitors," *Chem. Eng. J.*, vol. 470, no. 35, p. 144089, 2023, doi: 10.1016/j.cej.2023.144089.

[35] I. Falina, N. Loza, M. Brovkina, E. Titskaya, S. Timofeev, and N. Kononenko, "Electrotransport properties of perfluorinated cation-exchange membranes of various thickness," *Membranes (Basel)*, vol. 13, no. 11, 2023, doi: 10.3390/membranes13110873.

[36] M.A.A. Mohamed, M. Adel, and J. El Nady, "Evaluation of the electrochemical energy storage performance of symmetric supercapacitor devices based on eco-friendly synthesized nitrogen-doped graphene-like derivative electrodes from the perspective of their nanostructural characteristics," *Energy Adv.*, pp. 2947–2964, 2024, doi: 10.1039/d4ya00526k.

[37] J.H. Bang, B.H. Lee, Y.C. Choi, H.M. Lee, and B.J. Kim, "A study on superior mesoporous activated carbons for ultra power density supercapacitor from biomass precursors," *Int. J. Mol. Sci.*, vol. 23, no. 15, 2022, doi: 10.3390/ijms23158537.

[38] M.S. Islam, S.M. Hoque, M. Rahaman, M.R. Islam, A. Irfan, and A. Sharif, "Superior cyclic stability and capacitive performance of cation- and water molecule-preintercalated δ-MnO2/h-WO_3 Nanostructures as supercapacitor electrodes," *ACS Omega*, vol. 9, no. 9, pp. 10680–10693, 2024, doi: 10.1021/acsomega.3c09236.

[39] A. Azizpour, N. Bagovic, N. Ploumis, K. Mylonas, D. Hoxha, and F. Kienberger *et al*., "Electrochemical analysis of carbon-based supercapacitors using finite element modeling and impedance spectroscopy," *Energies*, vol. 18, no. 6, pp. 1–20, 2025, doi: 10.3390/en18061450.

[40] K. Gajewska, A. Moyseowicz, D. Minta, and G. Gryglewicz, "Effect of electrolyte and carbon material on the electrochemical performance of high-voltage aqueous symmetric supercapacitors," *J. Mater. Sci.*, vol. 58, no. 4, pp. 1721–1738, 2023, doi: 10.1007/s10853-023-08148-5.

[41] H. Wang, H. Niu, H. Wang, W. Wang, X. Jin, and H. Wang *et al*., "Micro-meso porous structured carbon nanofibers with ultra-high surface area and large supercapacitor electrode capacitance," *J. Power Sources*, vol. 482, no. June 2020, p. 228986, 2021, doi: 10.1016/j.jpowsour.2020.228986.

[42] G. Singh, Y. Kumar, and S. Husain, "Improved electrochemical performance of symmetric polyaniline/activated carbon hybrid for high supercapacitance: Comparison with indirect capacitance," *Polym. Adv. Technol.*, vol. 32, no. 11, pp. 4490–4501, 2021, doi: 10.1002/pat.5451.

[43] P. De, J. Halder, C.C. Gowda, S. Kansal, S. Priya, and S. Anshu *et al*., "Role of porosity and diffusion coefficient in porous electrode used in supercapacitors – Correlating theoretical and experimental studies," *Electrochem. Sci. Adv.*, vol. 3, no. 1, pp. 1–15, 2023, doi: 10.1002/elsa.202100159.

[44] L. Stolz, M. Winter, and J. Kasnatscheew, "Practical relevance of charge transfer resistance at the Li metal electrode|electrolyte interface in batteries?," *J. Solid State Electrochem.*, no. 0123456789, pp. 11–14, 2024, doi: 10.1007/s10008-023-05792-4.

[45] J. Tang, R. Muchakayala, S. Song, M. Wang, and K.N. Kumar, "Effect of EMIMBF4 ionic liquid addition on the structure and ionic conductivity of LiBF4-complexed PVdF-HFP polymer electrolyte films," *Polym. Test.*, vol. 50, pp. 247–254, 2016, doi: 10.1016/j.polymertesting.2016.01.023.

[46] N. Hidayati and Munasir, "Study of electrical and thermal properties of PVA-nanosilica as a candidate for supercapacitor separators," *J. Phys. Conf. Ser.*, vol. 2110, no. 1, pp. 0–6, 2021, doi: 10.1088/1742-6596/2110/1/012012.

[47] Y. Zilong, T. Dachuan, L. Jian, and N. Zhongming, "Dependence of Li-ion Battery energy density on separator thickness," *Chinese Phys. C*, vol. 45, p. 124107, 2021.

[48] N. Flores-Diaz, F. De Rossi, A. Das, M. Deepa, F. Brunetti, and M. Freitag, "Progress of photocapacitors," *Chem. Rev.*, vol. 123, no. 15, pp. 9327–9355, 2023, doi: 10.1021/acs.chemrev.2c00773.

[49] T. He, R. Jia, X. Lang, X. Wu, and Y. Wang, "Preparation and Electrochemical performance of PVdF ultrafine porous fiber separator-cum-electrolyte for supercapacitor," *J. Electrochem. Soc.*, vol. 164, no. 13, pp. E379–E384, 2017, doi: 10.1149/2.0631713jes.